

Optimization of Sliding Wear Behaviour of AA2219 Nanohybrid Composite Using Box-Behnken Design

Riddhisha Chitwadgi^{1*}, B Siddesh¹, B Latha Shankar¹, B Adveesh¹, R Suresh² and Siddeshkumar N G³

¹Siddaganga Institute of Technology, Tumkur, Karnataka, India. E-mail: riddhishac14@gmail.com

²M. S. Ramaiah University of applied science, Bengaluru, Karnataka, India.

³Channabasaveshwara Institute of Technology, Gubbi, Tumkur, Karnataka, India.

Abstract

The wear performance of a nano hybrid aluminum metal matrix composite was investigated in this study with a special emphasis on the impact of heat treatment on dry sliding behaviour. The hybrid composite was made with Al 2219 alloy as the matrix phase, 2% nano boron carbide (nB_4C) as the principal reinforcement, and 2% molybdenum sulphide (MoS_2) as additive using the stir casting technique. At room temperature, Pin-on-Disc equipment was utilized to carry out the task of varying sliding distance and load. Wear rates were assessed and further improvised using Box-Behnken design of response surface methodology. It was found that most significant parameter was sliding distance followed by load and aging temperature. 500m sliding distance, 10N load, and 240oC aging temperature were the optimal conditions for minimum wear rate.

Keywords: AA2219; B_4C ; Aging; Wear rate; Box-Behnken design

1.0 Introduction

Because reciprocating and rotating relative movements are experienced by engines, braking systems, bearings, and other mechanical parts, wear becomes a critical consideration to address when designing these components. Materials to be used for these mechanical elements need to be very strong and highly resistant to wear, with constant frictional coefficient, found to be stable under temperature variation, resistant to corrosion, and seizure resistant. Metal matrix composites reinforced with Ceramics are an attractive solution to these needs, resulting in a variety of applications in the automotive and aerospace industries²⁷. Particulate metal matrix composites (pMMC) outweigh metal matrix composites (MMC) with continuous fibers because of problems such as fiber damage, microstructural heterogeneity, and fiber damage due to contact. Studies show that a typical pMMC friction lining requires a metallic

matrix, particles and friction additives. The matrix material used in pMMC affects mechanical, thermal, and corrosion resistance⁸. To enhance mechanical behaviour, wear resistance, and thermal strength hard particles, such as Al_2O_3 , Al_4C_3 , B_4C , MgO, mullite, SiC, Si_3N_4 , SiO_2 , TiC and TiB_2 , are added to MMCs^{21,2}. Additives such as MoS_2 , graphite and boron nitride are employed to present better damping, non-variable friction, and anti-seizure characteristics. pMMCs with aluminum as matrix material are extensively used in aerospace purposes owing to its low weight, elevated heat conducting capacity and good resistance to corrosion²⁹. In particular, Al alloy 2219 (AA 2219) is mainly used for airframe contact parts and fuel tanks on account of its high stiffness and strength, excellent formability, desirable resistance to breakage and higher weldability⁵. With good resistance to impact and wear, tall melting point of 2450°C and less weight, B_4C nano-particles are introduced as a reinforcing phase to improve the wear performance of AA 2219. B_4C is the third hardest material,

*Author for correspondence

but little research has focused on its effects on Al alloys. Being strong oxidation resistant, stable for temperature variation and with inherent lubricating properties, lamellar soft MoS₂ particles are used as solid lubricants in addition to reinforcement and matrix material^{20,6,25,14}. In addition, by forming a tribolayer on the interface, it promotes the reduction of mating wear¹⁹. In the literature, a variety of materials-related and operational parameters have been found to have a complex influence on material wear behaviour³. Particle-assisted grain refinement, work hardening, dislocation strengthening and particle interaction effects are all examples of how particle size affects mechanical properties^{18,30}. AA 2024 matrix composites reinforced with nano B₄C particles outperformed AA 2024 matrix composites in wear resistance at low load (20 N) and sliding speed (0.6 m/s)¹³. The wear characteristics of the micro and nano Al matrix composites reinforced with B₄C were studied⁴. Nano B₄C particle-reinforced Al MMCs had a considerably lower wear rate than their micro counterpart, which they ascribed to nanoparticle-assisted grain refinement⁴. Abdollahi et al¹. reported a similar result using mechanical milling and hot extrusion procedures to make nano B₄C reinforced AA 2024 composites¹⁰. looked at the impact of lubricant MoS₂ (1.3 mm) particles on micron-sized B₄C (90 nm) reinforced Al MMCs. The findings revealed that increasing the MoS₂ content of hybrid composites by up to 5% improves wear resistance significantly. Saravanakumar²² found same thing for AA 2219.

The above review concludes that the reinforcing material,

its percentage, size, temperature, treatment time, wettability, manufacturing technique, and heat treatment all affect the mechanical properties of Al-MMC^{11,9}. Given the lack of wear research on nanoparticle-reinforced hybrid AA composites, the integration of nano-ceramic particles and solid lubricant additives should significantly improve the wear resistance of Al-MMC. This is the goal of our current research, as well as to better understand how heat treatment affects these composites. Hybrid composite AA2219 was created using a stir casting process. The wear performance of these, is shown at a constant velocity of 3.77 m/s over a wide range of aging temperatures (200–2400°C), sliding lengths (500–1500m) and loads (10–50 N).

2.0 Materials Used

In this study, the matrix employed to fabricate the composites was AA 2219, an Al alloy. Its chemical configuration was obtained spectroscopically and is found in Table 1. The mechanical and other properties of the materials are shown in Table 2.

A two-step stir casting procedure was adopted to prepare the AA2219 hybrid nano-composites reinforced with n-B₄C and MoS₂ particulates both 2% by weight. The particle sizes of B₄C and MoS₂ were 30-60 nm and 600-900 nm respectively. Ethane (C₂H₆) tablet was used as degassing agent. As the name of the method suggests, particles were added to the melt in two phases. In the first stage, the Al

Table 1: Chemical configuration of AA 2219

Elements	Mg	Si	Cu	Zr	Fe	Zn	Ti	V	Zn	Al
Weight in%	0.020	0.20	6	0.2	≤0.30	≤0.10	0.06	0.1	≤0.1	Remaining

Source: <https://asm.matweb.com/search/SpecificMaterial.asp?bassnum=ma2219t62>



Figure 1: Specimen in the furnace



Figure 2: Wear experimental set up



Figure 3: Specimen on the disc

Table 2: Properties of materials

Properties of AA 2219	Value
Density (in g/cm ³)	2.54
Strength in tension (in MPa)	172-476
Elasticity modulus (in GPa)	73.8

Source: <https://alloysintl.com/inventory/aluminum-alloys/aluminium2219/>, <https://asm.matweb.com/search/SpecificMaterial.asp?bassnum=ma2219t62>

alloy melt was added to the n-B₄C and K₂TiF₆ slurry, and the mixture was vigorously stirred for 5-8 minutes in the speed range of 200 to 250 rpm. The MoS₂ particles were then mixed with the melt-generated vortices to achieve uniform dispersion and actively swirl in the second stage. The molten melt was then poured into a cast iron mold preheated to 300°C. and air cooled to room temperature.

3.0 Research Methodology

3.1 Age Hardening of Composites

The age-hardening technique was used to heat treat the composites. In a Muffle furnace, the age-hardening process was carried out at three distinct temperatures: 200°C, 220°C, and 240°C. The samples were steeped for 24 hours after reaching the proper temperature, then air cooled. Figure 1 shows this set-up.

3.2 Wear Test

As shown in Figure 2, the pins of a disc tribometer unit (model TR 20LE-PHM-400, DUCOM, India) are used for dry sliding wear testing. Hardened 8mm diameter x 30mm high pin specimens were tested using a 120mm diameter EN-31 steel rotating disc. This is shown in Figure 3. The chemical composition (in per cent) of the steel disc was: Carbon is 0.15%, Manganese is 0.8%, Silicon is 0.26%, and S and P are 0.04%. The disc had a tensile strength of 430 MPa, a hardness of 62 HRC and a surface roughness of 1.6 Ra.

No lubrication was used in any of the wear tests. Dry sliding wear testing was done as per the ASTM G 99-05 standard. After each experiment, ultrasonic cleaning of samples was done using acetone, then they were dried and checked for weight using a digital balance (METTLER, accuracy: 0.01 mg). The specific rate of wear in mm³ N/m of the composites was evaluated by density (g/mm³), sliding distance (m), and mass loss (g) due to applied load (N). The morphology of wear surface of the composites was studied to better understand the processes that may occur under

different values of factors namely; sliding distance, temperature and loading condition. Three repetitions were considered, and average of results of each test were calculated.

3.3 Box Behnken Design

Response Surface Methodology (RSM) is a statistic based method for modeling, refining, and optimizing the response variable with a limited number of tests. Traditional experiment design, in which one component is altered at a time, involves the use of a large number of resources, and despite this, assessing the cumulative effects of the applied parameters is challenging^{10,7}. Taguchi Technique, Grey Relational Analysis, RSM, evolutionary techniques and hybrid techniques are used in literature for optimizing the wear behaviour of Al MMCs^{28,16,17,12}. In this work Box Behnken Design (BBD) of RSM is adopted for optimization of the response variable. The advantage behind using this method is that this design demands each factor to be studied at three levels only and also avoids use of extreme points¹⁵.

A full explanation of the factor selection procedure was presented in previous work²⁵ and it was found that sliding speed had the least effect on wear rate of the four factors evaluated. As a result, decision was made to include the critical properties of load, aging temperature and sliding distance, as the least important factor was excluded from the current study and the focus is on the effect of aging temperature on wear performance. To fit a second-order polynomial to the response surface, a 3-level BBD for each factor was chosen from the general design in RSM. To determine the error for the three selected variables and three levels of, the design requires 15 trials with 12 factor points and 3 center points. The ingredients and amounts used in the experiments are found in Table 3, and the trials were performed in the order of the design matrix given in Table 4. A quadratic regression model is set up to predict this relationship. Equation (1) gives the general form, where, Y is the response variable, x_i and x_j are the input factors, b_0 is the intercept; b_j , b_{jj} , and b_{ij} are interaction coefficients; k

Table 3: Design Parameters and their values used

Factors	Units	Factor Levels		
		-1	0	+1
Aging Temperature (AT)	Degree Celsius	200	220	240
Sliding Distance (SD)	Meters	500	1000	1500
Load (L)	Newtons	10	30	50

Table 4: Design Matrix for wear tests

Standard Order	Run Order	Aging temperature (AT)	Sliding distance (SD)	Load (L)	Material Removal (cm ³)
1	1	-1	-1	0	0.00805
2	2	+1	-1	0	0.00527
11	3	0	-1	+1	0.00051
14	4	0	0	0	0.00581
13	5	0	0	0	0.00584
6	6	-1	0	-1	0.01355
9	7	0	-1	-1	0.00793
10	8	0	+1	-1	0.00372
3	9	-1	+1	0	0.00505
4	10	+1	+1	0	0.00548
7	11	-1	0	+1	0.00145
15	12	0	0	0	0.01375
5	13	-1	0	-1	0.00139
8	14	+1	0	+1	0.00432
12	15	0	+1	+1	0.00766

Table 5: Analysis of Variance Results

Source	DF	Sum of squares.	Mean square.	F value.	PValue.
Model.	9	3.5×10 ⁻⁵	0.4×10 ⁻⁵	19.20	0.002
Linear	3	3.3×10 ⁻⁵	1.1×10 ⁻⁵	54.68	0.000
AT (°Celsius)	1	0.5×10 ⁻⁵	0.5×10 ⁻⁵	23.20	0.005
SD (m)	1	1.8×10 ⁻⁵	1.8×10 ⁻⁵	89.18	0.000
L (N)	1	1×10 ⁻⁵	1×10 ⁻⁵	51.65	0.001
Square	3	0.1×10 ⁻⁸	0.1×10 ⁻⁸	0.61	0.638
AT (°Celsius)* AT (°Celsius)	1	0.1×10 ⁻⁸	0.1×10 ⁻⁸	0.52	0.503
SD (m)* SD (m)	1	0.1×10 ⁻⁸	0.1×10 ⁻⁸	1.38	0.292
L(N)*L(N)	1	0.1×10 ⁻⁸	0.1×10 ⁻⁸	0.00	0.948
2-Way interaction	3	0.1×10 ⁻⁵	0.1×10 ⁻⁸	2.33	0.192
AT (°Celsius)* SD (m)	1	0.1×10 ⁻⁵	0.1×10 ⁻⁵	2.53	0.172
AT (°Celsius)* L (N)	1	0.1×10 ⁻⁸	0.1×10 ⁻⁸	0.55	0.491
SD (m)* L (N)	1	0.1×10 ⁻⁵	0.1×10 ⁻⁸	3.89	0.106
Error	5	0.1×10 ⁻⁵	0.1×10 ⁻⁸		
Lack-of-fit	3	0.1×10 ⁻⁵	0.1×10 ⁻⁸		
Pure error	2	0.1×10 ⁻⁸	0.1×10 ⁻⁸		
Total	14	3.6×10 ⁻⁵			

representing number of parameters, equals to 3 in this study and the term gives the error.

$$Y = b_0 + \sum_{j=1}^k b_j x_j + \sum_{j=1}^k b_{jj} x_j^2 + \sum_i \sum_{<j=2}^k b_{ij} x_i x_j + e_i \dots (1)$$

4.0 Results and Discussion

4.1 Analysis of Variance

The results of wear rate analysis are reported in Table 5. Less than 0.05 p-value indicates that the terms are important. Here, individual process parameters – AT, SD, L are all significant model terms. The R² value obtained was 97.19 per cent and the R² (adjusted) was 92.13 per cent.

4.2 Contour Plot

A contour plot graphically represents a 3-Dimensional surface in 2D space using the third variable Z in the form of slices called contours. It is used to understand the relationship between two factors (say x and y) on the response variable z. It also shows the maximum, and minimum points and can be used for determining values of x and y which give the same or constant z values. The areas with the same z value are shaded.

Contour Plot of WEAR RATE vs SLIDING DISTANCE, AGEING TEMPERATURE

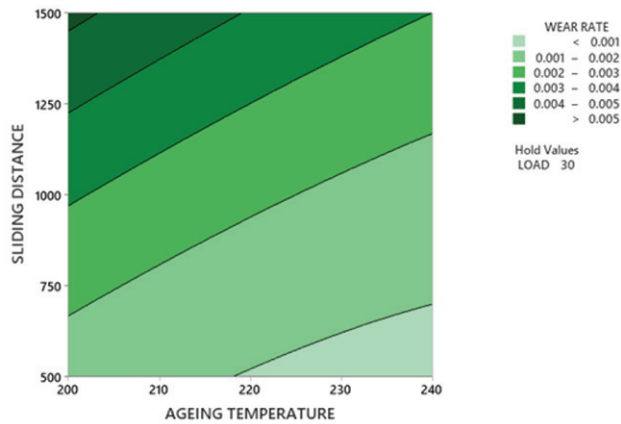


Figure 4: Contour plot for wear behaviour against aging temperature, sliding distance

Contour Plot of WEAR RATE vs LOAD, AGEING TEMPERATURE

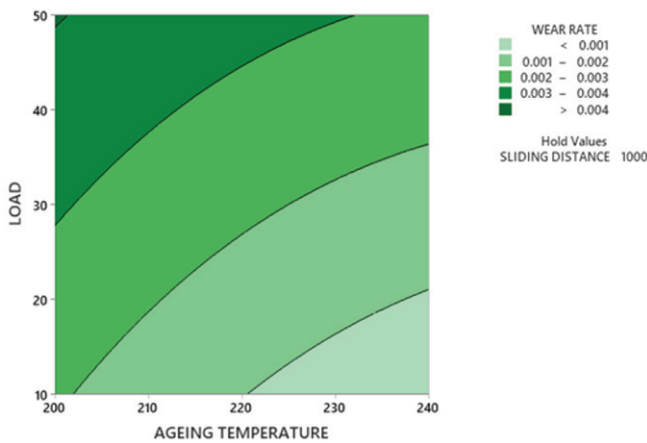


Figure 5: Contour plot for wear behaviour against aging temperature, load

Contour Plot of WEAR RATE vs LOAD, SLIDING DISTANCE

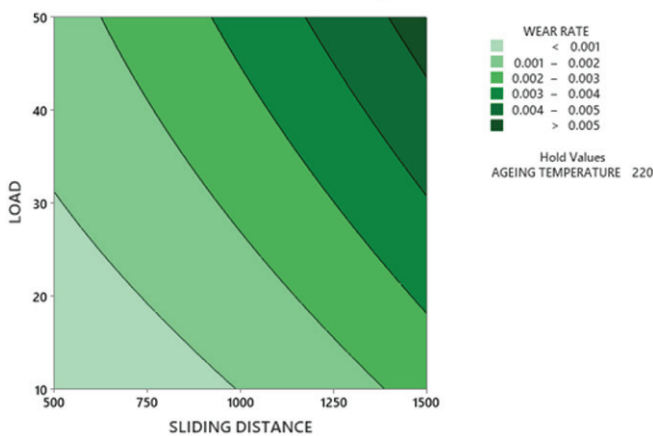


Figure 6: Contour plot for wear behaviour against load, sliding distance

The interaction effect of aging temperature and sliding distance on wear behaviour is depicted in Figure 4. From these contours shown, at the middle value of the load, less than 0.001 mm³/m of wear rate is observed at the maximum range of aging temperature of 220°C-240°C and at lower sliding distance up to 700m. Steep increment of wear rate is seen above 1000m of sliding distance when the aging temperature is within 220°C. It is evident from this discussion that greater values of aging temperature up to 240°C and lower sliding distance tend to reduce the wear loss for AA2219 hybrid nano-composites. Contour plot Figure 5 depicts the influence of aging temperature and load on wear rate. At 1000m of sliding distance and at applied load, the wear rate reduces with the aging temperature up to 240°C. Less than 0.002 mm³/m of wear rate is observed at less than 20N of load for a range of aging temperatures equal to and beyond 210°C. At a maximum aging temperature of 240°C, lower values of load yielded an almost meagre wear rate for 2219 hybrid nano-composites. This is consistent with the results put forth by earlier researchers²¹.

The combined influence of load and sliding distance upon wear rate is shown in the contour plot in Figure 6. Sliding distance up to 1000m does not have any influence upon wear rate when the load is at lower range of 10 to 20N. Maximum wear rate happens at higher values of the sliding distance of 1500m and 50 N of load.

It is apparent that AA2219 hybrid nano-composites show better wear behaviour at lower values of sliding distance and load. Other researchers also reported the same trend of increase in wear rate with load and sliding distance in Al MMCs^{26,18}.

4.3 Correlation with Regression Analysis

A polynomial regression equation of second-order to predict the wear rate as provided by regression analysis is given in equation 2.

$$\begin{aligned} \text{Wear rate (m}^3\text{/Nm)} &= 0.0235 - .000200 \times \text{AT} \\ &+ .000007 \times \text{SD} - .000076 \times \text{L} + .0000001 \times \text{AT} \times \text{AT} \\ &+ .0000002 \times \text{SD} \times \text{SD} - .0000001 \times \text{L} \times \text{L} - .0000002 \\ &\times \text{AT} \times \text{SD} + .0000002 \times \text{AT} \times \text{L} + .0000003 \times \text{SD} \times \text{L} \dots (2) \end{aligned}$$

4.4 Optimization

This study was carried out based on “smaller the better,” concept considering that composite with the lowest wear rate as the best. Table 6 gives the ideal settings for the lowest wear rate obtained by multi-response prediction. It was concluded that ideal specifications for the lowest wear rate are given by an aging temperature of 240°C, a load of 10 N and a sliding distance of 500m.

Table 6: Optimized solution for wear rate

Solution	AT (°Celsius)	SD (m)	L (N)	Wear Rate (m ³ /Nm)	Composite Desirability
1	240	500	10	-0.0001567	1

5.0 Conclusions

Following important conclusions are drawn from the present investigation;

Two-phase stir casting method can be successfully adopted for the fabrication of AA2219 particulate nano composites reinforced with 2% weight n-B₄C and 2% weight MoS₂.

ANOVA analysis yielded the relative significance of the various parameters that influence the wear performance of alloy and accordingly can be organised in the order: Sliding distance > Load > Aging temperature.

Lower values of sliding distance, reduced values of load, and higher values of aging temperature result in lower wear rates, as shown by the contour plots.

Sliding distance : 500m, Load : 10N, Aging temperature: 240°C are the parametric values at which the response is optimum.

A regression equation was developed that estimated the wear rate with 92% accuracy, and predicted and measured wear data correlated with +5% error. These results confirm that estimated model has the ability to explain the wear data with a reasonable level of precision.

6.0 References

1. Abdollahi, A., Alizadeh, A. and Baharvandi, H.R. (2014): In: Proceedings Materials & Design, 55, p.471.
2. Chandio, A.D., Ansari, M.B., Hussain, S. and Siddiqui, M.A., (2019): Silicon carbide effect as reinforcement on aluminium metal matrix composite. *Journal Chemical Society of Pakistan*, 41(4), pp.650-654.
3. Dev P, Charoo MS. (2018): Role of reinforcements on the mechanical and tribological behaviour of aluminum metal matrix composites – a review. *Mater Today Proc* 2018; 5: 20041-53.
4. Harichandran R. and Selvakumar N. (2016): 'Effect of nano/micro B₄C particles on the mechanical properties of aluminum metal matrix composites fabricated by ultrasonic cavitation-assisted solidification process. *Areli. Cir Mecli. Eiiğ*. 2016. 16. 147.158.
5. Kennedy F.E., Balbahadur A.C... Lashmore D.C, The friction, and wear of Cu-based silicon carbide particulate metal matrix composites for brake applications *Wear* 203-204 (1987) 715-721.
6. Khakbiz M. and Akhlaghi F. (2009): 'Synthesis and structural characterization of Al-B₄C nano-composite powders by mechanical alloying'. *Journal of Alloys and Compounds* 2009, 479. 334-34 1.
7. Khuri, A.I. and Mukhopadhyay, S., (2010): Response surface methodology. *Wiley Interdisciplinary Reviews: Computational Statistics*, 2(2), pp.128-149.
8. Kim J.D., Kim H.J., Koh S.W. (2006): Wear characteristics of particulate reinforced metal matrix composites fabricated by a pressureless metal infiltration process, *Mater. Sci. Forum* 510-511 (2006) 234-237.
9. Koksai, S., Ficici, F., Kayikci, R. and Savas, O., (2012): Experimental optimization of dry sliding wear behaviour of in situ AlB₂/Al composite based on Taguchi's method. *Materials & Design*, 42, pp.124-130.
10. Kumar, R. and Dhiman, S., (2013): A study of sliding wear behaviours of Al-7075 alloy and Al-7075 hybrid composite by response surface methodology analysis. *Materials & Design*, 50, pp.351-359.
11. Lashgari, H.R., Zangeneh, S., Shahmir, H., Saghafi, M. and Emamy, M., (2010): Heat treatment effect on the microstructure, tensile properties and dry sliding wear behaviour of A356-10% B₄C cast composites. *Materials & Design*, 31(9), pp.4414-4422.
12. Madhukar, P., Selvaraj, N., Mishra, V., Rao, C.S.P. (2020): Optimization of Wear Parameters of AA7150-TiC Nano-composites by Taguchi Technique. In: Dutta, D., Mahanty, B. (eds) *Numerical Optimization in Engineering and Sciences. Advances in Intelligent Systems and Computing*, vol 979.
13. Mistry J.M, Gohil P.P. (2018): Science and Engineering of Composite Materials, 25(4)(2018) 633-47.
14. Miyajima, T. and Iwai, Y., (2003): Effects of reinforcements on sliding wear behaviour of Aluminum matrix composites. *Wear*, 255(1-6), pp.606-616.
15. Montgomery, D.C., (2017): Design and analysis of experiments. John Wiley & sons.
16. Poovalingam Muthu, (2021): Multi objective optimization of wear behaviour of Aluminum MMCs using Grey Taguchi method. *Manufacturing Rev.*, 7, 2020, pp.1-8.

17. Ravikumar, M., Reddappa, H., N., Suresh R Babu E R and Nagaraja, C R, (2022): Optimization of wear behaviour of Al7075/SiC/Al₂O₃ MMCs Using statistical method. *Advances in Materials and Processing Technologies*, pp.1-18.
18. Ravindranath VM, Shankar GSS, Basavarajappa S, Kumar NGS. (2017): Dry sliding wear behaviour of hybrid aluminum metal matrix composite reinforced with boron carbide and graphite particles. *Mater Today Proc* 2017;4:11163-7.
19. Riahi, A.R. and Alpas, A.T., (2001): The role of tribolayers on the sliding wear behaviour of graphitic aluminum matrix composites. *Wear*, 251(1-12), pp.1396-1407.
20. Rouhi, M., Moazami-Goudarzi, M. and Ardestani, M., (2019). Comparison of effect of SiC and MoS₂ on wear behaviour of Al matrix composites. *Transactions of Nonferrous Metals Society of China*, 29(6), pp.1169-1183.
21. Roy, M., Venkataraman, B., Bhanuprasad, V.V., Mahajan, Y.R. and Sundararajan, G., (1992): The effect of particulate reinforcement on the sliding wear behaviour of aluminum matrix composites. *Metallurgical Transactions A*, 23(10), pp.2833-2847.
22. Saravanakumar, V.B. huveneswari, G. Gokul (2020): *Materials Today Proceedings*, 27(2020) 2645-2649.
23. Shankar, B. Latha, K. C. Anil, and Rahul Patil. (2016): "A study on 3-body abrasive wear behaviour of aluminium 8011/graphite metal matrix composite." In *IOP Conference Series: Materials Science and Engineering*, vol.149, no.1, p.012099. IOP Publishing.
24. Shankar, B. Latha, P. M. Nagaraj, and K. C. Anil. "Optimization of wear behaviour of AA8011-Gr composite using Taguchi technique." *Materials Today: Proceedings* 4, no. 10 (2017): 10739-10745.
25. Siddesh Kumar, N.G., Ram Prabhu, T., Shiva Shankar, G.S. and Basavarajappa, S., (2016): Dry sliding wear properties of unhybrid and hybrid Al alloy based nano-composites. *Tribology-Materials, Surfaces & Interfaces*, 10(3), pp.138-149.
26. Siddesh Kumnar N. G., Shiva Shankar G. S. and Basavarajappa S. (2015): 'A study on dry sliding wear behaviour of hybrid metal matrix composites at room temperature, *Applied Mechanics and Materials*, 766, 219-228.
27. Umanath, K.P.S.S.K., Palanikumar, K. and Selvamani, S.T., (2013): Analysis of dry sliding wear behaviour of Al6061/SiC/Al₂O₃ hybrid metal matrix composites. *Composites Part B: Engineering*, 53, pp.159-168.
28. Velavan, K., Palanikumar, K. and Senthilkumar, N., (2021): Experimental investigation of sliding wear behaviour of boron carbide and mica reinforced aluminium alloy hybrid metal matrix composites using Box-Behnken design. *Materials Today: Proceedings*, 44, pp.3803-3810.
29. Velmurugan, C., Subramanian, R., Ramakrishnan, S.S., Thirugnanam, S., Kannan, T. and Anandavel, B., (2014): Experimental investigations on the effect of heat-treatment parameters on the wear behaviour of aluminum hybrid composites. *Industrial Lubrication and Tribology*.
30. Zhang Z. and Chen D. L. 2008: 'Contribution of Orowan strengthening effect in particulate-Reinforced metal matrix nano-composites'. *Mate; Sdy. Eng.*, A. 483-484. 148.152.